J. V. C. Vargas
Department of Mechanical Engineering and Materials Science, Duke University, Durham, NC 27708-0300

M. Sokolov
Department of Fluid Mechanics and Heat Transfer, Tel-Aviv University, Ramat-Aviv 69978 Israel

A. Bejan
Department of Mechanical Engineering and Materials Science, Duke University, Durham, NC 27708-0300

Thermodynamic Optimization of Solar-Driven Refrigerators

This paper describes the thermodynamic optimization of a class of refrigerators without work input, which are driven by heat transfer from a solar collector. The model consists of a finite-size solar collector with heat loss to the ambient, and a refrigerator with three finite-size heat exchangers, namely, the evaporator between refrigeration load and refrigerant, the condenser between the refrigerant and the ambient, and the heat exchanger between the solar collector and the refrigerant. The total thermal conductance of the three heat exchangers is fixed. The solar collector heat loss to the ambient is proportional to the collector-ambient temperature difference. The first part of the paper reports the operating conditions for maximum refrigeration effect, specifically, the optimal collector temperature, and the optimal way of allocating the thermal conductance inventory to the three heat exchangers. For example, the optimal condenser conductance is equal to half of the total thermal conductance, and is independent of other operating parameters. The second part of the paper examines the changes in the optimal design when the price of the refrigeration load (p_L) is different (higher) than the price of the heat input provided by the collector (p_H). The optimal collector temperature and the optimal three-way allocation of the thermal conductance inventory are reported as functions of the price ratio p_H/p_L.

1 Introduction

The method of entropy generation minimization has emerged during the last two decades as a distinct subfield in heat transfer (e.g., Bejan, 1982, 1996). The method consists of the simultaneous application of heat transfer and thermodynamics principles in the pursuit of realistic models of heat transfer processes, devices, and installations. By "realistic" models we mean models that account for the inherent irreversibility of heat, mass, and fluid flow processes. In engineering, the entropy generation minimization method is known also as thermodynamic optimization and thermodynamic design. It has been applied extensively, for example, to the optimization of the storage and retrieval of solar energy (e.g., Adebiyi and Russell, 1987; Krane, 1987; Charach, 1993; Bellecci and Conti, 1994).

The importance and growth of this field are further illustrated by the emergence of a similar activity more recently in physics. The physics work is usually referred to as thermodynamics in finite time (e.g., Andresen et al., 1984), and its methodology is precisely the same combination of heat transfer and thermodynamics. Some of the most fundamental results refer to the optimization of power plants and refrigeration plants with heat transfer irreversibilities. In the power generation area, the focus was on the regime for the production of maximum instantaneous power (Chambadal, 1957; Novikov, 1957; El-Wakil, 1962, 1971; Curzon and Ahlborn, 1975), which is equivalent to the regime of minimum entropy generation rate (see Bejan, 1996, pp. 227–232).

In the refrigeration area the models that have been optimized based on this method had power input and heat rejection to the ambient (Bejan, 1989), as in the case of the vapor compression cycle (Klein, 1992; Radcenco et al., 1994). They were optimized by maximizing the refrigeration load (rate of heat extraction from the cold space), which is the same as minimizing the rate of entropy generation of the cold space of the refrigeration plant. In this paper we consider the fundamentals of the thermodynamic optimization of solar driven refrigeration plants, i.e., refrigerators without work input (Bejan et al., 1995). The heat input Q_H is provided at the temperature level T_H by a flat-plate solar collector, Fig. 1. The objectives of this study are to determine: (1) The operating conditions for maximum refrigeration effect, and (2) the optimal way of dividing a finite supply of heat exchanger surface between the three heat exchangers of the refrigeration plant.

Heat-driven refrigerators constitute an important class both, fundamentally, because of the peculiarity of almost no work input, and, practically, because the driving heat transfer (Q_H in Fig. 1) can be low grade heat, e.g., solar (Sokolov and Hershgal, 1993) or waste heat. The utilization of low-grade heat sources is stressed by environmental and economic considerations. Such optimization is crucial for low grade and low efficiency solar systems. For this reason we apply the present method to the optimization of a refrigerator driven by heat transfer from a solar collector.

2 Model With Heat Transfer Irreversibilities

In a heat-driven refrigerator the working fluid executes cycles while removing the refrigeration load Q_L from the refrigerated space T_L, and rejecting the heat transfer Q_0 to the ambient T_0. The cycle is driven by the heat transfer Q_H received from the source temperature T_H. There is no work transfer between the refrigerator and its environment.

From the outset, we recognize that the refrigerator operates irreversibly because of several entropy generating mechanisms that are always present, for example, heat transfer, throttling, and mixing (Sokolov and Hershgal, 1991). In the model shown on Fig. 1, we have divided the refrigerator into five compartments, the solar collector, the three heat exchangers (Q_H, Q_0, Q_L) and the rest of the refrigeration plant. The solar collector has two heat transfer irreversibilities (Bejan et al., 1981): the net heat transfer from the sun to the collector, and the heat leak from the collector to the ambient. The solar collector and the three heat exchangers account for the irreversibility of the machine, and the remaining components are modeled as irreversibility free. The (C) label used in Fig. 1 is an allusion to Carnot's name, to

Contributed by the Solar Energy Division of THE AMERICAN SOCIETY OF MECHANICAL ENGINEERS for publication in the ASME JOURNAL OF SOLAR ENERGY ENGINEERING. Manuscript received by the ASME Solar Energy Division, Dec. 1994; final revision, Sept. 1995. Associate Technical Editor: W. M. Worek.

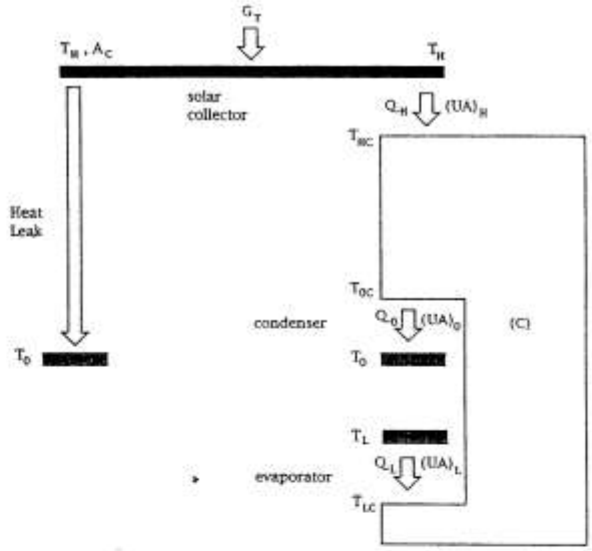

Fig. 1 Model with heat transfer irreversibilities for an irreversible refrigerator driven by a solar collector with heat loss to the ambient

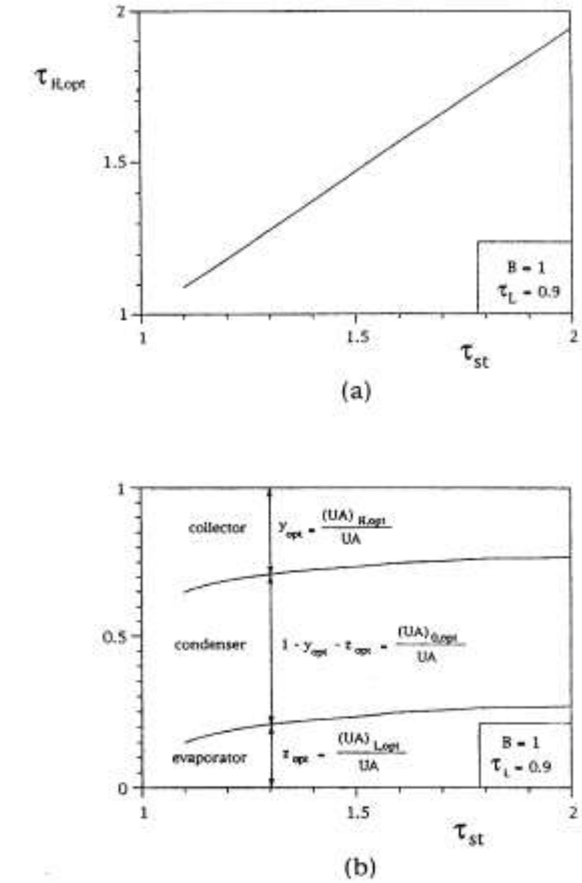

Fig. 2 (a) The effect of the stagnation temperature (τ_{st}) on the optimal collector heat exchanger temperature; (b) the effect of the stagnation temperature (τ_{st}) on the optimal allocation of thermal conductance among the three heat exchangers

suggest a system that operates reversibly. This label is not meant to suggest that a Carnot refrigerator (with work transfer) resides in the indicated compartment.

In summary, in the following analysis we neglect the irreversibility associated with frictional pressure drops, throttling, and mixing. This assumption is consistent with the treatment of power plants (Novkiov, 1957; El-Wakil, 1962, 1971; Curzon and Ahlborn, 1975; Bejan, 1988) and refrigeration plants based on the vapor compression cycle (Klein, 1992; Radcenco et al., 1994).

The compartments of the irreversible refrigerator and collector model are described analytically by the six statements:

$$Q_H = A_C G_T [a - b(T_H - T_0)] \tag{1}$$

$$Q_H = (UA)_H (T_H - T_{HC}) \tag{2}$$

$$Q_0 = (UA)_0 (T_{0C} - T_0) \tag{3}$$

$$Q_L = (UA)_L (T_L - T_{LC}) \tag{4}$$

$$\frac{Q_H}{T_{HC}} + \frac{Q_L}{T_{LC}} = \frac{Q_0}{T_{0C}} \tag{5}$$

$$Q_H + Q_L = Q_0 \tag{6}$$

where A_C is the collector area, G_T is the irradiance at the collector surface, and a and b are two constants that can be calculated as shown by Sokolov and Hershgal (1993). Equation (1) represents a flat-plate collector with partial heat loss to the ambient. The group $[a - b(T_H - T_0)]$ is known as the collector efficiency, and

$$T_{st} = T_0 + \frac{a}{b} \tag{7}$$

is the stagnation (i.e., the ceiling) temperature of the collector. When $T_H = T_{st}$ the heat output Q_H is zero. Sokolov and Hershgal (1993) demonstrated that when the collector and heat exchanger are specified, there exists an optimal collector temperature for maximum refrigeration effect, i.e., an optimal *coupling* between the solar collector and the refrigerator. However, Sokolov and

Nomenclature

- a = constant, K
- b = constant
- A = heat transfer area, m^2
- A_C = collector area, m^2
- B = dimensionless group, Eq. (12)
- G_T = irradiance on collector surface, W/m^2
- p_H = price of heat input, dollars/W
- p_L = price of refrigeration load, dollars/W
- P = profit function, dollars, Eq. (21)
- Q_H = heat input, W
- Q_L = refrigeration load, W
- Q_0 = condenser heat transfer, W
- $\mathbf{R}$ = residual vector
- T_H = collector heat exchanger temperature, K
- T_{HC} = hot-end temperature of reversible compartment, K, Fig. 1
- T_L = refrigeration load temperature, K
- T_{LC} = cold-end temperature of the reversible compartment, K, Fig. 1
- T_{st} = collector stagnation temperature, K
- T_0 = ambient temperature, K
- T_{0C} = intermediate temperature of the reversible compartment, K, Fig. 1
- U = overall heat transfer coefficient based on A, W/(m^2 K)
- y = conductance fraction, Eq. (19)
- z = conductance fraction, Eq. (19)
- τ = dimensionless temperatures defined as T/T_0
- $(\ )_C$ = reversible compartment
- $(\ )_H$ = collector heat exchanger
- $(\ )_L$ = evaporator
- $(\ )_{opt}$ = optimum
- $(\ )_0$ = ambient
- $(\sim)$ = dimensionless variable

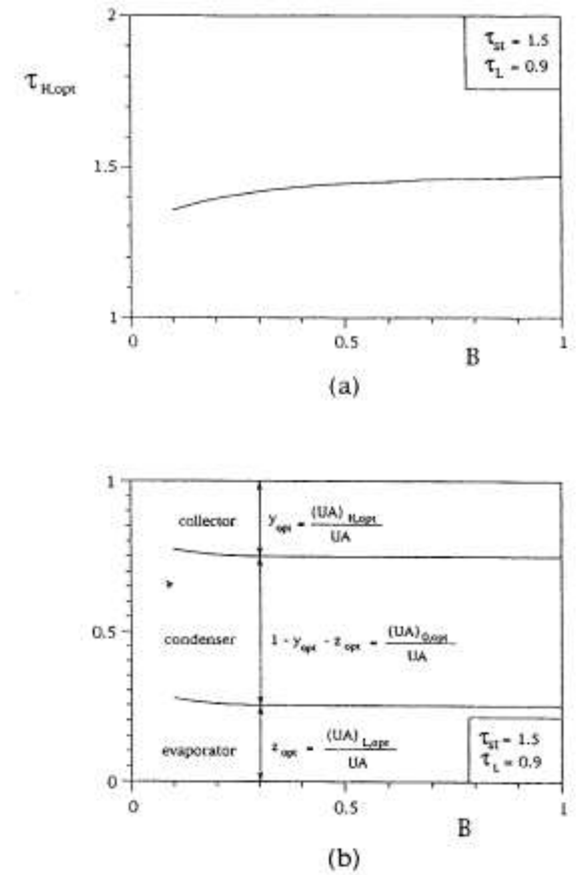

Fig. 3 (*a*) The effect of the collector size (B) on the optimal collector heat exchanger temperature; (*b*) the effect of the collector size (B) on the optimal allocation of thermal conductance among the three heat exchangers

Hershgal (1993) did not perform a resources optimization. They assumed a given resources distribution and optimized the coupling temperature. What is proposed here is to first optimize the distribution of finite resources and then the coupling temperature. This way, a total optimization which is so critical for low efficiency systems may be accomplished.

Each factor of type UA in Eqs. (2)–(4) represents the overall thermal conductance of the respective heat exchanger, or the product between the heat transfer area A and the overall heat transfer coefficient U based on A. The thermal conductances $(UA)_H$, $(UA)_0$ and $(UA)_L$ are assumed constant, i.e., independent of temperature. They are rough measures of the sizes (amounts of hardware) of the three heat exchanges, therefore a reasonable economic constraint (e.g. Bejan, 1988, p. 409) is

$$UA = (UA)_H + (UA)_0 + (UA)_L, \quad \text{(constant)} \tag{8}$$

which states that the total thermal conductance inventory UA is fixed. The question on which we focus in the following analysis is how to divide the UA inventory between $(UA)_H$, $(UA)_0$ and $(UA)_L$, such that the refrigeration rate Q_L is maximized. The total thermal conductance constraint has been used extensively in the thermodynamic optimization of irreversible power generation and refrigeration models, as reviewed in Bejan (1996).

We first write the problem statement using the following appropriate nondimensional groups:

$$\tau_H = \frac{T_H}{T_0}, \quad \tau_L = \frac{T_L}{T_0} \tag{9}$$

$$\tau_{HC} = \frac{T_{HC}}{T0}, \quad \tau_{0C} = \frac{T_{0C}}{T_0}, \quad \tau_{LC} = \frac{T_{LC}}{T_0} \tag{10}$$

$$\tilde{Q}_H = \frac{Q_H}{UAT_0}, \quad \tilde{Q}_0 = \frac{Q_0}{UAT_0}, \quad \tilde{Q}_L = \frac{Q_L}{UAT_0} \tag{11}$$

$$\tau_{st} = \frac{T_{st}}{T_0}, \quad B = \frac{bA_C G_T}{UA}. \tag{12}$$

The B parameter describes the size of the collector relative to the cumulative size of the collector heat exchanger, condenser, and the evaporator. The resulting dimensionless equations are

$$\tilde{Q}_H = B(\tau_{st} - \tau_H) \tag{13}$$

$$\tilde{Q}_H = y(\tau_H - \tau_{HC}) \tag{14}$$

$$\tilde{Q}_0 = (1 - y - z)(\tau_{0C} - 1) \tag{15}$$

$$\tilde{Q}_L = z(\tau_L - \tau_{LC}) \tag{16}$$

$$\frac{\tilde{Q}_H}{\tau_{HC}} + \frac{\tilde{Q}_L}{\tau_{LC}} = \frac{\tilde{Q}_0}{\tau_{0C}} \tag{17}$$

$$\tilde{Q}_H + \tilde{Q}_L = \tilde{Q}_0. \tag{18}$$

Note that Eqs. (13)–(18) deliver $\tilde{Q}_L$ as a function of six dimensionless numbers, B, τ_{st}, τ_H, τ_L, y, and z, where y and z are the conductance allocation ratios

$$y = \frac{(UA)_H}{UA}, \quad z = \frac{(UA)_L}{UA}. \tag{19}$$

Note also that according to the UA constraint (8), the equipment fraction allocated to the condenser is

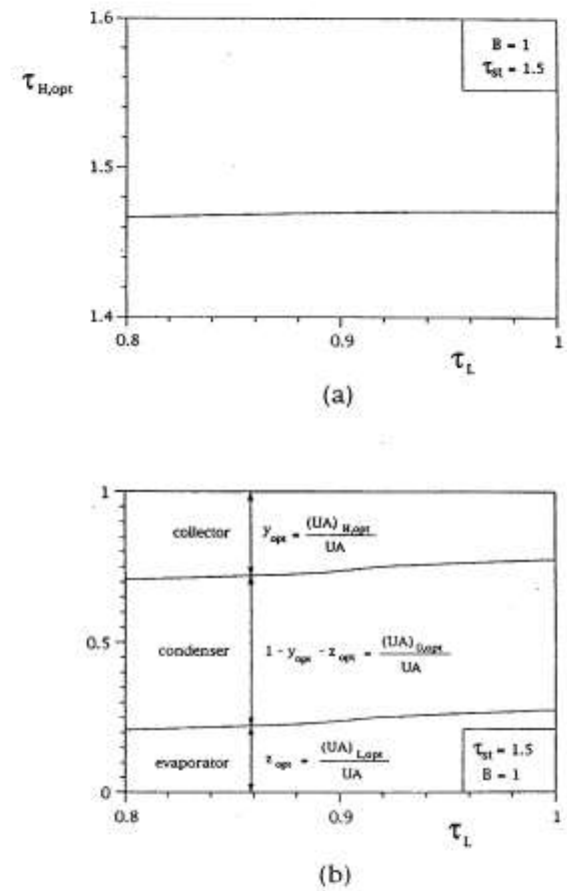

Fig. 4 (*a*) The effect of the refrigerated space temperature (τ_L) on the optimal collector heat exchanger temperature; (*b*) the effect of the refrigerated space temperature (τ_L) on the optimal allocation of thermal conductance among the three heat exchangers

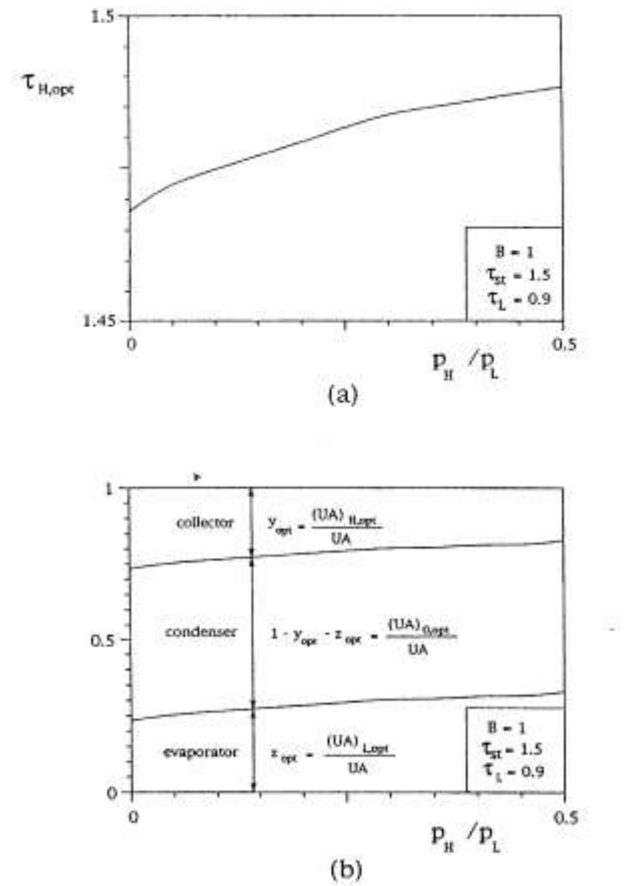

Fig. 5 (*a*) The effect of the price ratio (p_H/p_L) on the optimal collector heat exchanger temperature ($B = 1$, $\tau_{st} = 1.5$, $\tau_L = 0.9$); (*b*) the effect of the price ratio (p_H/p_L) on the optimal allocation of thermal conductance among the three heat exchangers ($B = 1$, $\tau_{st} = 1.5$, $\tau_L = 0.9$)

$$\frac{(UA)_0}{UA} = 1 - y - z. \tag{20}$$

3 The Effect of the Cost of the Heat Input

The optimization described so far was based on maximizing the refrigeration load Q_L. This choice is appropriate only when the cost of the heat input Q_H is negligible when compared with the economic value of the refrigeration effect Q_L. In general, however, the heat input is not available freely, and the relevant objective function to maximize is the profit

$$P = p_L Q_L - p_H Q_H. \tag{21}$$

Here p_L and p_H are the known prices of the refrigeration load and the heat input. We are interested in dividing the total UA inventory of Eq. (8) such that P is maximized.

The problem statement consists of Eqs. (1)–(5), (7), (8), and (21). We write the nondimensionalized profit function as

$$\tilde{P} = \frac{P}{p_L UAT_0} = \tilde{Q}_L - \frac{p_H}{p_L}\tilde{Q}_H \tag{22}$$

which depends on B, τ_{st}, τ_H, τ_L, y, z, and p_H/p_L. In summary, the nondimensional equations for this problem are (13)–(18) and (22).

4 Numerical Method and Results

The numerical problem consisted of solving the nonlinear system (13)–(18) to maximize $\tilde{Q}_L$. Equation (22) was introduced later to maximize $\tilde{P}$. Some selected parameters were held constant and others were varied to generate the results shown in Figs. 2–7. Each point on the plotted curves was determined as the solution of the above system of equations for a set of fixed parameters (τ_H, τ_{st}, B, τ_L, y, z). Once the set of fixed parameters is defined, Eqs. (13) and (14) deliver τ_{HC}, and the system of Eqs. (15)–(18) and (22) is solved for $\tilde{P}$, $\tilde{Q}_0$, $\tilde{Q}_L$, τ_{0C}, and τ_{LC}. This system is represented in compact form by the residual vector $\mathbf{R} = 0$. A Newton-Raphson method with appropriate initial guesses was used for both maximization problems. A tolerance for the Euclidian norm of the residual vector $|\mathbf{R}|_2 \le 10^{-8}$ was imposed to achieve convergence in all solutions. We have used as initial guess the last converged solution for the previous set of fixed parameters. In this way convergence was achieved with little computational time.

For the first part of the problem, we maximized $\tilde{Q}_L$, holding B, τ_{st}, and τ_L constant, and varying τ_H, y, and z. The set of optimal values ($\tau_{H,opt}$, y_{opt}, z_{opt}) that maximizes $\tilde{Q}_L$ is reported in Figs. 2–4 for several combinations of B, τ_{st}, and τ_L. In ejector refrigeration cycle applications the refrigeration load is extracted from temperatures T_L ranging from −15°C to 5°C (Sokolov and Hershgal, 1991). This range is represented approximately by $\tau_L = 0.9$, which has been used to develop the numerical results shown in Figs. 2–7.

Figures 2(*a*), 3(*a*) and 4(*a*), show that $\tau_{H,opt}$ increases monotonically as τ_{st}, B and τ_L increase. It is worth noting that in Fig. 2(*a*) $\tau_{H,opt}$ is consistently greater than $\tau_{st}^{1/2}$; i.e., greater than the optimal collector temperature determined by Bejan et al. (1981) for a collector coupled to a power cycle that has

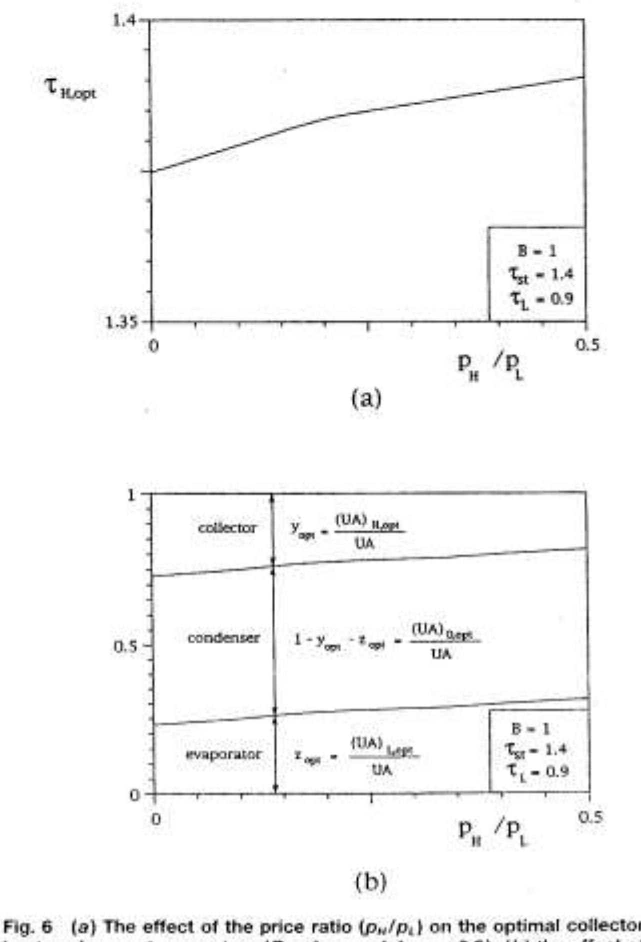

Fig. 6 (*a*) The effect of the price ratio (p_H/p_L) on the optimal collector heat exchanger temperature ($B = 1$, $\tau_{st} = 1.4$, $\tau_L = 0.9$); (*b*) the effect of the price ratio (p_H/p_L) on the optimal allocation of thermal conductance among the three heat exchangers ($B = 1$, $\tau_{st} = 1.4$, $\tau_L = 0.9$)

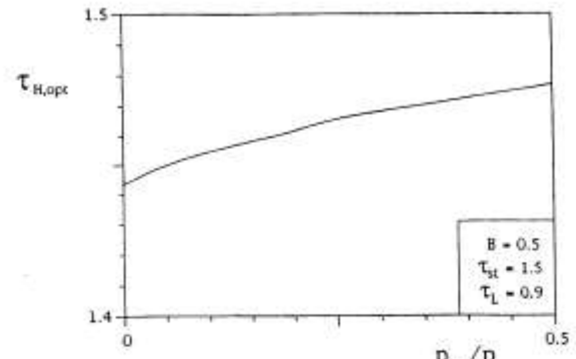

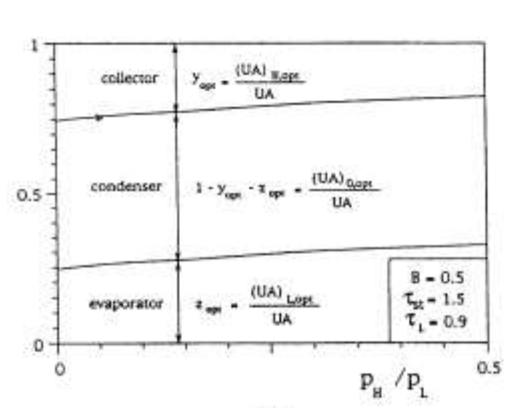

Fig. 7 (*a*) The effect of the price ratio (p_H/p_L) on the optimal collector heat exchanger temperature ($B = 1$, $\tau_{st} = 1.5$, $\tau_L = 0.9$); (*b*) the effect of the price ratio (p_H/p_L) on the optimal allocation of thermal conductance among the three heat exchangers ($B = 0.5$, $\tau_{st} = 1.5$, $\tau_L = 0.9$)

no heat transfer irreversibilities, and by Sokolov and Hershgal (1993) for collector coupled with a reversible refrigeration cycle. Figure 3(a) shows the effect of the collector size (B) on the optimal collector temperature. We see that the collector temperature increases only slightly as the B parameter increases by a factor of 10 (from 0.1 to 1). Figure 4(a) shows that the τ_L variation has a negligible effect on the optimal collector temperature.

The results plotted in Fig. 2(b) show y_{opt} and z_{opt} in a way that illustrates the splitting of the total thermal conductance (an amount equal to 1 on the ordinate) between the collector heat exchanger, condenser, and evaporator. We see that the condenser demands half of the total thermal conductance, regardless of the external temperature levels (τ_H, τ_L) and B. Figures 2(b) and 4(b) show that $(UA)_{L,opt}$ increases at the expense of $(UA)_{H,opt}$ as both τ_{st} and τ_L increase. In Fig. 3(b) we see that $(UA)_{L,opt}$ decreases only slightly as B increases from 0.1 to 1.

In the second part of the numerical work, we maximized $\tilde{P}$ by varying τ_H, y, and z while holding B, τ_{st}, τ_L and p_H/p_L constant. The set of optimal values ($\tau_{H,opt}$, y_{opt}, z_{opt}) that maximizes $\tilde{P}$ is reported in Figs. 5–7 for several combinations of B, τ_{st}, τ_L and p_H/p_L. Note that the limit $p_H/p_L = 0$ represents the Q_L maximization results obtained in the first part of the study.

Figures 5(a), 6(a), and 7(a) show that $\tau_{H,opt}$ increases monotonically as the price ratio p_H/p_L increases. The most striking feature is that the condenser demands half of the total thermal conductance, regardless of the price ratio p_H/p_L and the external temperature levels (τ_H, τ_L) and the collector size (B). In other words, the conclusion reached earlier is more general. In Figs. 5(b), 6(b) and 7(b) we see that $(UA)_{L,opt}$ increases at the expense of $(UA)_{H,opt}$ as the price ratio p_H/p_L increases. The group B has a negligible effect on the conductance allocation fractions y_{opt} and z_{opt}: this effect is illustrated in Figs. 5(b) and 7(b) where B decreases from 1 to 0.5.

5 Conclusions

In this paper we presented the thermodynamic optimization of solar-driven refrigeration plants without work input. This was based on a model (Fig. 1) that accounted for the irreversibility of the plant and solar collector, the finiteness of the heat exchanger inventory (total thermal conductance), and the finiteness of the collector. We determined the operating regime for maximum refrigeration effect, and how the optimal performance is affected by the collector size and the extreme temperature levels of the refrigeration plant (Figs. 2–4).

From a practical standpoint, the most important conclusion is that the maximum refrigeration regime requires that the thermal conductance be allocated in a certain way between the three heat exchangers. The allocation of the thermal conductance is influenced to some extent by the relative price of the heat source (Figs. 5–7). The optimal thermal conductance of the ambient-temperature heat exchanger is half of the total supply, and is relatively independent of the price of the heat source.

Acknowledgment

This work was supported by the National Science Foundation, Conselho Nacional de Desenvolvimento Cientifico e Tecnologico–CNPq (Brazil), Tel Aviv University, and a travel grant to Israel from the Ministry of Science and Arts of Israel. A preliminary report on this collaborative project was presented by Bejan (1994).

References

Adebiyi, G., and Russell, L. D., 1987, "A Second Law Analysis of Phase-Change Thermal Energy Storage Systems," *ASME HTD*, Vol. 80, pp. 9–20.

Andresen, B., Salamon, P., and Berry, R. S., 1984, "Thermodynamics in Finite Time," *Phys. Today*, Sept., pp. 62–70.

Bejan, A., Kearney, D. W., and Kreith, F., 1981, "Second Law Analysis and Synthesis of Solar Collector Systems," ASME Journal of Solar Energy Engineering, Vol. 103, pp. 23–30.

Bejan, A., 1982, *Entropy Generation through Heat and Fluid Flow*, John Wiley and Sons, New York.

Bejan, A., 1988, *Advanced Engineering Thermodynamics*, John Wiley and Sons, New York.

Bejan, A., 1989, "Theory of Heat Transfer-Irreversible Refrigeration Plants," *Int. J. Heat Mass Transfer*, Vol. 32, pp. 1631–1639.

Bejan, A., 1994, "Second Law Aspects of Solar Thermal Energy Conversion," *International Conference on Comparative Assessments of Solar Power Technologies (SOLCOM-1)*, Jerusalem, Feb. 14–18.

Bejan, A., 1996, *Entropy Generation Minimization*, CRC Press, Boca Raton, FL.

Bejan, A., Vargas, J. V. C., and Sokolov, M., 1995, "Optimal Allocation of a Heat-Exchanger Inventory in Heat Driven Refrigerators," *Int. J. Heat Mass Transfer*, Vol. 38, pp. 2997–3004.

Belleci, C., and Conti, M., 1994, "Phase Change Energy Storage: Entropy Production, Irreversibility and Second Law Efficiency," *Solar Energy*, Vol. 53, pp. 163–170.

Charach, Ch., 1993, "Second Law Efficiency of an Energy Storage-Removal Cycle in a Phase-Change Material Shell-and-Tube Heat Exchanger," ASME Journal of Solar Energy Engineering, Vol. 115, pp. 240–243.

Chambadal, P., 1957, *Les Centrales Nucleaires*, Armand Colin, Paris, pp. 41–58.

Curzon, F. L., and Ahlborn, B., 1975, "Efficiency of a Carnot Engine at Maximum Power Output," *Am. J. Phys.*, Vol. 43, pp. 22–24.

El-Wakil, M. M., 1962, *Nuclear Power Engineering*, McGraw-Hill, New York, pp. 162–165.

El-Wakil, M. M., 1971, *Nuclear Energy Conversion*, International Textbook Company, Scranton, PA, pp. 31–35.

Klein, S. A., 1992, "Design Considerations for Refrigeration Cycles," *Int. J. Refrig.*, Vol. 15, pp. 181–185.

Krane, R. J., 1987, "A Second Law Analysis of the Optimum Design and Operation of Thermal Energy Storage Systems," *Int. J. Heat Mass Transfer*, Vol. 30, pp. 43–57.

Novikov, I. I., 1958, "The Efficiency of Atomic Power Stations," *J. Nuclear Energy II*, Vol. 7, pp. 125–128; translated from *Atomnaya Energiya*, 1957, Vol. 3, No. 11, p. 409.

Radcenco, V., Vargas, J. V. C., Bejan, A., and Lim, J. S., 1994, "Two Design Aspects of Defrosting Refrigerators," *Int. J. Refrig.*, Vol. 18, pp. 76–86.

Sokolov, M., and Hershgal, D., 1991, "Operational Envelope and Performance Curves for a Compression-Enhanced Ejector Refrigeration System," *ASHRAE Trans.*, Vol. 97, No. 2, pp. 394–402.

Sokolov, M., and Hershgal, D., 1993, "Optimal Coupling and Feasibility of a Solar-Powered Year-Round Ejector Air Conditioner," *Solar Energy*, Vol. 50, pp. 507–516.